

# Modeling and Analysis of an Induction Machine Soft-Starter Interconnected to a Power Cable Using Frequency Domain Equivalents

Jose de Jesus Chavez, M. Madrigal, Pedro Garcia-Vite

**Abstract**—This paper presents the modeling of a induction machine soft-starter interconnected to a power cable configuration for transient analysis through frequency domain technique using circuit equivalents. The entirely network is partitioned into linear and nonlinear subnetworks. In this work, the power cable and the induction machine are taken as linear elements and their equivalents are obtained. Meanwhile, the soft starter device, composed by a silicon-controlled rectifier (SCR), is taken as a non linear element. An iterative procedure is conducted at the interconnected bus for all subnetworks. Afterwards, the whole network including equivalent elements, is solved via the Numerical Laplace transform. The methodology is able to provide steady and dynamic state signals. Results of a case of study were corroborated with PSCAD simulations.

**Index Terms**—Electromagnetic transients, Laplace transforms, frequency domain analysis, soft-start/induction machine, power cables.

## I. INTRODUCTION

COMMONLY, electric power networks are composed of several dynamic elements with complex interactions among them. The accuracy in the modeling of the elements of a power network depends on the nature of the phenomenon and study requirements to perform as well as the chosen methodology. The analysis and modeling of these networks often require the use of equivalent and/or simulation tools representing the system behavior in a manner suitable for the required studies. For instance, in studies as a power-flow, simplified models are enough for the analysis. While, in short-term high-frequency events analysis detailed models of individual elements are indispensable, including saturated and switching elements.

Time domain (TD) [1], frequency domain (FD) [2], and to a lesser extent hybrid domain analysis [3] are generally the main methodologies (mature and well-proven) used to simulate electric power networks. TD methods consist on a sequential solution scheme of integro-differential equations; the nature

of the methodology allows the straightforward inclusion of switching and saturated elements. While, elements such as power cables, transmission lines and transformers hold a high frequency dependence being the FD the ideal methodology for the analysis. The methodology used in this paper belongs to the class of hybrid techniques mixing time and frequency domain models overcoming the intrinsic errors that present the techniques alone.

In this work, linear frequency dependent networks are modeled as Norton/Thevenin equivalents in FD and nonlinear networks are modeled in TD. A Newton type procedure is used to join both methodologies. The response of the whole network is evaluated in the frequency domain, but time domain solution is found using inverse transformation algorithms such as the Numerical Laplace Transform (NLT). The hybrid time/frequency technique leads to efficient, robust periodic dynamic state solutions for the entirely network.

In this paper the hybrid methodology of the frequency domain equivalents (FDE) is applied to an AC voltage-controlled based on soft starter induction machine interconnected to an undersea power cable. AC voltage-controlled soft starters offer many advantages over conventional starters. By reducing the applied voltage; smooth acceleration and energy savings are achieved [4]. Also by this way, the core and stator losses can be reduced. Nevertheless, harmonic losses in the motor and SCR are introduced. Computational time savings are achieved using the FDE methodology especially on higher density networks, as the case of study.

The main sections of the paper are organized as follows. In section II, the basic concepts of the methodology are presented. It is also addressed, in this section an illustrative example. In section III, the case of study is presented. In addition, the optimization of the soft start AC voltage controller used is explained. Conclusions are drawn in section IV.

## II. BASIC CONCEPTS

The main concepts of the hybrid methodology used to simulate the AC-voltage controlled soft-started induction machine connected to an offshore electric network are addressed in this section. It is worth mentioning that the methodology presented in this section is non-unique for this kind of networks and can be extended and used for any network configuration.

### A. Solution Procedure

- The network under study is partitioned at the nodes of interest or arbitrarily in N-subnetworks.

---

This work was supported in part by the Faculty Improvement Program of Mexico (PROMEP) Folio: ITMOR-PTC-005, Clearance letter: PROMEP/103.5/12/3679.

J. J. Chavez and M. Madrigal are with the Graduate Program of Electrical Engineering at the Morelia Technological Institute, Morelia Michoacan Mexico (e-mail of corresponding author: jjchavez@itmorelia.edu.mx, and manuelmadrigal@itmorelia.edu.mx).

P. Garcia-Vite is with the University Polytechnic of Altamira, Altamita Tamaulipas Mexico (e-mail: pedro.garcia@upalt.edu.mx).

Paper submitted to the International Conference on Power Systems Transients (IPST2013) in Vancouver, Canada July 18-20, 2013.

- Linear loads and frequency-dependent elements establish one or more subnetworks.
- Nonlinear elements with high participation in the network and/or specific nonlinear elements formed other M-subnetworks.
- Assumed an initial flat voltage in each partition buses ( $V_{k,old} = 1pu$ ).
- FD Norton equivalent networks are obtained for each linear/frequency-dependent N-subnetwork [2].
- The Jacobians are obtained at M-nonlinear (time variant) elements/subnetworks from their characteristic differential equations through local TD technic.
- Linear and non-linear Jacobians are added. A new voltage ( $V_{k,new}$ ) is obtained by a Newton type procedure, this process be carried out until a default convergence is reached.
- Once the voltages/currents at the interface nodes are obtained, one can move deeper into each subnetwork for calculating any internal variable under interest.
- The inverse NLT, is used to transform signals from FD to TD. For further details about the LT please see the appendix I.

The solution methodology above presented is diagrammatically outlined in Fig. 1 accompanied with the main equations.

### B. Illustrative Example

To validate the proposed methodology this section provides an illustrative example. Fig. 2 shows a single-phase bridge-rectifier supplied by a 120V, 60Hz source ( $v_s$ ). The values of the linear time invariant elements are:  $R = 500\Omega$ , and  $C = 126.2\mu F$ . In addition, the diode resistances are  $0.01\Omega$  and  $1 \times 10^5\Omega$ , for on and off states, respectively.

According to the previous section, the network is partitioned in 2 subnetworks. Where, the subnetwork 1 correspond to the nonlinear element (diode D) and the subnetwork 2 to the linear time invariant elements (R and C). After, the linear Jacobian is obtained from the subnetwork 2 ( $J_L$ ). Later in all nodes of partition, it is assumed a start voltage ( $V_{A,old}$ ). The Jacobian of the nonlinear network ( $J_{NL}$ ) and the current  $I_{NL}$  are calculated using a local TD solution. While, the linear subnetwork current is calculated with  $I_L = J_L V_{A,old}$ . After all, a Newton type procedure is conducted until the convergence is reached. A simulation of 0.9s was performed and the signals obtained by the frequency domain equivalent (FDE) methodology at the partition node ( $V_A$ ) were obtained and compared against those obtained by PSCAD® to corroborate the accuracy of the methodology. Voltages and currents are shown on Fig. 3 (a) and (b), respectively. A good approximation is observed between the PSCAD and FDE methods throughout the simulation time. The calculated percentage of error in the voltage is 0.3164% and occurs at the moment when the diode change from on to off state (see the zoom on Fig. 3 (a)). Although this is an illustrative example the reader can realize the ability and accuracy of the methodology.

### III. CASE OF STUDY

Fig. 4 shows the schematic diagram of the case of study. Physically, it consist of two offshore platforms interconnected

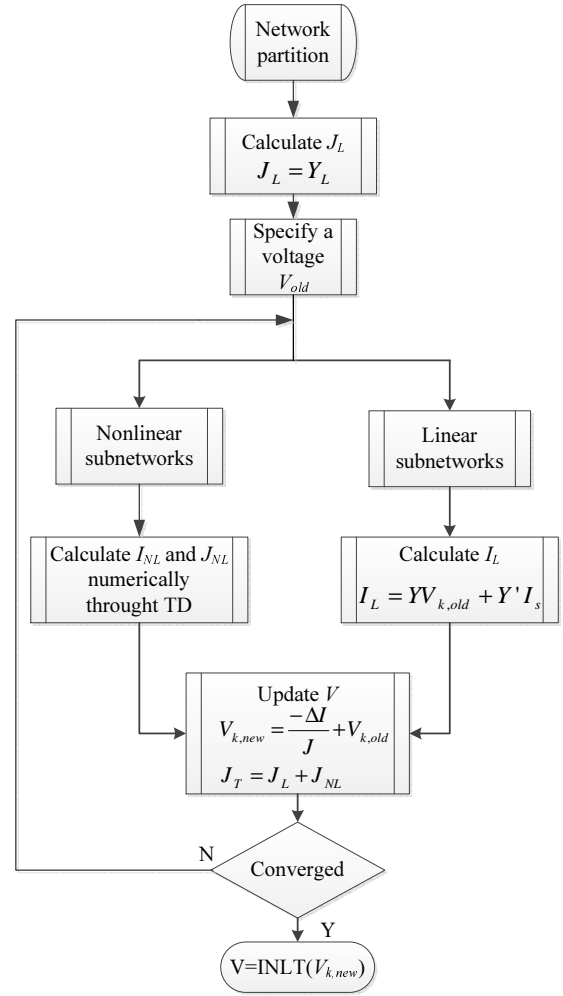


Fig. 1. Flowchart of the methodology.

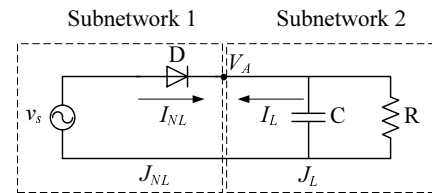
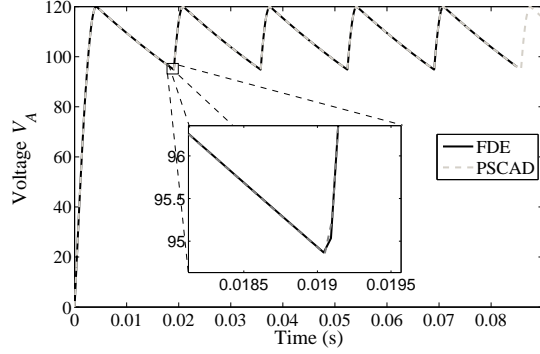
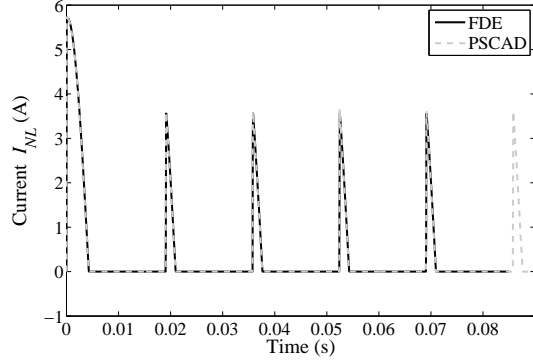


Fig. 2. Single-phase bridge-rectifier.

through a 20km undersea power cable. At both ends of the power cable a linear transformer is connected (for simplicity in this paper, saturation is not taken into account, but the methodology can be readily extended to overcome this kind of effects). Electrical energy is produced in one of the platforms and delivered to 20km far away on the other platform where a group of linear loads and a 500hp induction machine (IM) are connected. The IM is connected to the network by an AC voltage control based on SCR. Following the methodology described above, the network is partitioned into subnetworks as seen on Fig. 4. The FDEs are calculated for linear and frequency dependent elements. While, the nonlinear elements are solved by a local TD (see Fig. 4b).

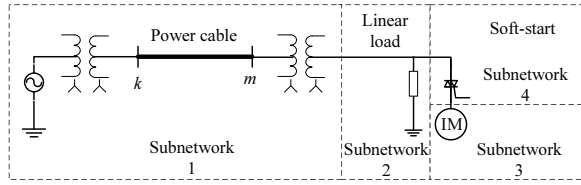


(a)

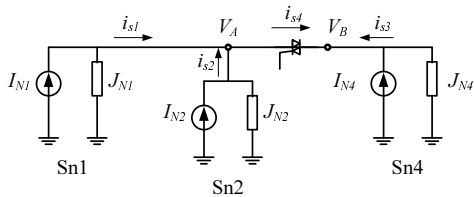


(b)

Fig. 3. Signals comparisons FDE vs PSCAD: (a) Voltage at the partitioned bus  $V_A$  and (b) current through the diode  $i_{NL}$ .



(a)



(b)

Fig. 4. Case of study: (a) Full representation, (b) subnetwork partitions and their equivalents.

#### A. Subnetwork 1: Power Cable

The first subnetwork (Sn1) is composed by three main elements: an excitation source, two transformers connected at each end of the cable, and the power cable at itself. The source and the transformers are taken as linear elements while the power cable belongs to the frequency dependent elements.

The model of the power cable is based on of coaxial loops [5]. Then, the series impedances are calculated by the following set of loop equations.

$$-\begin{bmatrix} \frac{dV_1}{dx} \\ \frac{dV_2}{dx} \\ \frac{dV_3}{dx} \end{bmatrix} = \begin{bmatrix} Z_{11} & Z_{12} & 0 \\ Z_{21} & Z_{22} & Z_{23} \\ 0 & Z_{32} & Z_{33} \end{bmatrix} \begin{bmatrix} I_1 \\ I_2 \\ I_3 \end{bmatrix}. \quad (1)$$

Instead of the loop voltage and current obtained through Eq. 1, are necessary currents and voltages of the core, sheath, and armor. By introducing appropriate conditions in Eq. 1 terminals necessary signals are obtained by [1]:

$$-\begin{bmatrix} \frac{dV_{core}}{dx} \\ \frac{dV_{sheath}}{dx} \\ \frac{dV_{armor}}{dx} \end{bmatrix} = \begin{bmatrix} Z_c & Z_{cs} & Z_{ca} \\ Z_{sc} & Z_s & Z_{sa} \\ Z_{ac} & Z_{as} & Z_a \end{bmatrix} \begin{bmatrix} I_{core} \\ I_{sheath} \\ I_{armor} \end{bmatrix}. \quad (2)$$

The power cable characteristic impedance ( $Z_c$ ) and propagation function ( $\gamma$ ) are given by [1]:

$$Z_c(\omega) = \sqrt{\frac{Z(\omega)}{Y(\omega)}} \quad \gamma(\omega) = \sqrt{Z(\omega)Y(\omega)}. \quad (3)$$

The two ports representation for the power cable is given by [6]:

$$\begin{bmatrix} I_{km} \\ I_{mk} \end{bmatrix} = \begin{bmatrix} A & -B \\ -B & A \end{bmatrix} \begin{bmatrix} V_k \\ V_m \end{bmatrix}, \quad (4)$$

where

$$A = Y_c \coth(\gamma(\omega)l), \quad B = Y_c \operatorname{csch}(\gamma(\omega)l),$$

$l$  is the length of the power cable and the subscripts  $k$  and  $m$  represent both ends of the power cable (see Fig. 4). Further details of the power cable modeling can be found on [1].

Eq. 4 is arranged to include the transformers and excitation source

$$\begin{bmatrix} I_s \\ I_m \end{bmatrix} = \begin{bmatrix} Y_{T1} + A & -B \\ -B & A + Y_{T2} \end{bmatrix} \begin{bmatrix} V_k \\ V_A \end{bmatrix}, \quad (5)$$

where  $I_s$  is the current of the excitation source and  $Y_{T1}$ ,  $Y_{T2}$  correspond to the linear transformers, whose impedance is given by  $Z_{T1} = R + sL$ . The values used in this paper for the linear elements where summarised in appendix III. Then a frequency domain Norton equivalent is obtained to represent the subnetwork 1.

#### B. Subnetwork 2: Linear Load

In the receiving offshore platform, a three-phase balanced linear load is connected to the network via bus ( $V_A$ ). Being the linear load characteristic equation is:

$$Z = R + sL. \quad (6)$$

The FDEs resulting for each linear or frequency dependent subnetwork are evaluated during the entire frequency spectrum ( $N = \frac{T}{\Delta t}$ ). Even though inherent numerical problems such as aliasing and Gibbs oscillation are presented at the NLT have been alleviated using data windows and other oscillation techniques (for further details about the NLT see [8]).

#### C. Subnetwork 3: Induction Machine

The steady-state representation of an IM is based on the assumption that the network to which it is connected is balanced and linear.

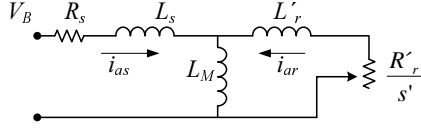


Fig. 5. Conventional equivalent circuit for steady-state behavior of induction machines.

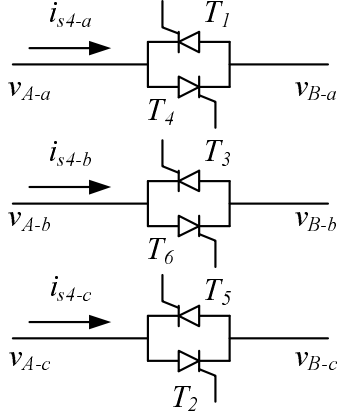


Fig. 6. Antiparallel thyristor controllers.

Fig. 5 shows the well-known equivalent circuit for the balance steady-state behavior of a three phase induction machine. The single representation is used in phases  $a, b, c$  provided there is only one winding of the field structure.

$$\begin{bmatrix} V_B \\ 0 \end{bmatrix} = \begin{bmatrix} R_s + sL_s + sL_M & -sL_M \\ -sL_M & sL_r + \frac{R'_r}{s'} + sL_M \end{bmatrix} \begin{bmatrix} I_{as} \\ I_{ar} \end{bmatrix} \quad (7)$$

where  $s'$  is the slip of the IM. The subscripts  $s$  and  $r$  are referred to stator and rotor, respectively. For a  $s' = 0.5$  the steady-state current of the IM is  $1 \times 10^{-3}$  pu.

However this is not the best approximation when it is needed to study the performance of the drive during transients [1]. Nevertheless, when it is needed to simulate the induction machine drive with switching networks, it is not wise enough to describe the whole drive system through equations for various modes of operation.

#### D. Subnetwork 4: SCR

In this subnetwork three SCRs are placed in series with the IM (see Fig. 6). Due to the behavior of the switching devices this subnetwork is considered as a nonlinear subnetwork. Respective voltages and currents are obtained by a local TD procedure that solved the characteristic differential equations. At each one of the thyristor the current can be varied from a maximum value (thyristor valves bypassed) to a zero conduction (thyristor valves open) by varying the thyristor's firing angle  $\alpha$  within the range  $90^\circ < \alpha < 180^\circ$ .

The SCR is modeled as a low/high resistance for an on/off state of the thyristors. The resistors are  $0.01\Omega$  and  $1 \times 10^5\Omega$

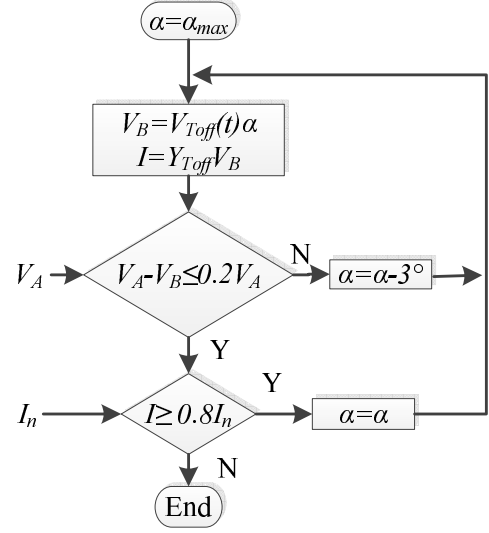


Fig. 7. Optimal AC Voltage Soft Start control.

for on/off respectively. The simulation results of the network with and without the soft start voltage controlled during 0.55s are shown in Fig. 8. Fig. 8(a), without the soft start device or full voltage supply shows the current through the stator. It is noticed that the magnitude of the current is nearly  $2 \times 10^{-3}$  pu during the first seconds (two times the steady state magnitude). Also, tends to steady-state slowly. On Fig. 8(b), it is shown the simulation of the system with the soft start voltage controller. The maximum magnitude of the current is reached at the first half cycle regardless the fire angle. After the second positive half wave the conduction angle is increased by a determine factor until the specific limit is reached. Even when the conduction angle changes in each cycle, it is seen that the steady-state is reached faster than the simulation without soft star device. The methodology takes into account any signal change during the simulation time at the partitioned nodes.

#### E. Optimal AC Voltage Soft Start Controlled

From Fig. 9, it can be seen the behavior of the voltage and current during the optimal soft started voltage-controller. The soft started voltage-controlled begins with the thyristors fired at an  $\alpha$  equal to  $\alpha_{max}$ . When the motor is stand still, the voltage across the nonconducting thyristor is measured [7]. The voltage across the nonconducting thyristor is the difference between the excitation voltage ( $V_A$ ) and the  $emf$  ( $V_B$ ). Then,  $\alpha$  is decremented by  $3^\circ/cycle$  while the next expression is not satisfied (see Fig. 9(a)):

$$V_A - V_B \leq 0.2V_A. \quad (8)$$

The fundamental component of the line current drawn is monitored every  $\Delta t$ . If the current is less than the current limit, then  $\alpha$  is decremented by  $3^\circ/cycle$  until the identification of the end of soft start is reached as shown in Fig. 9(b). If the current exceeds the current limit, then  $\alpha$  will not be

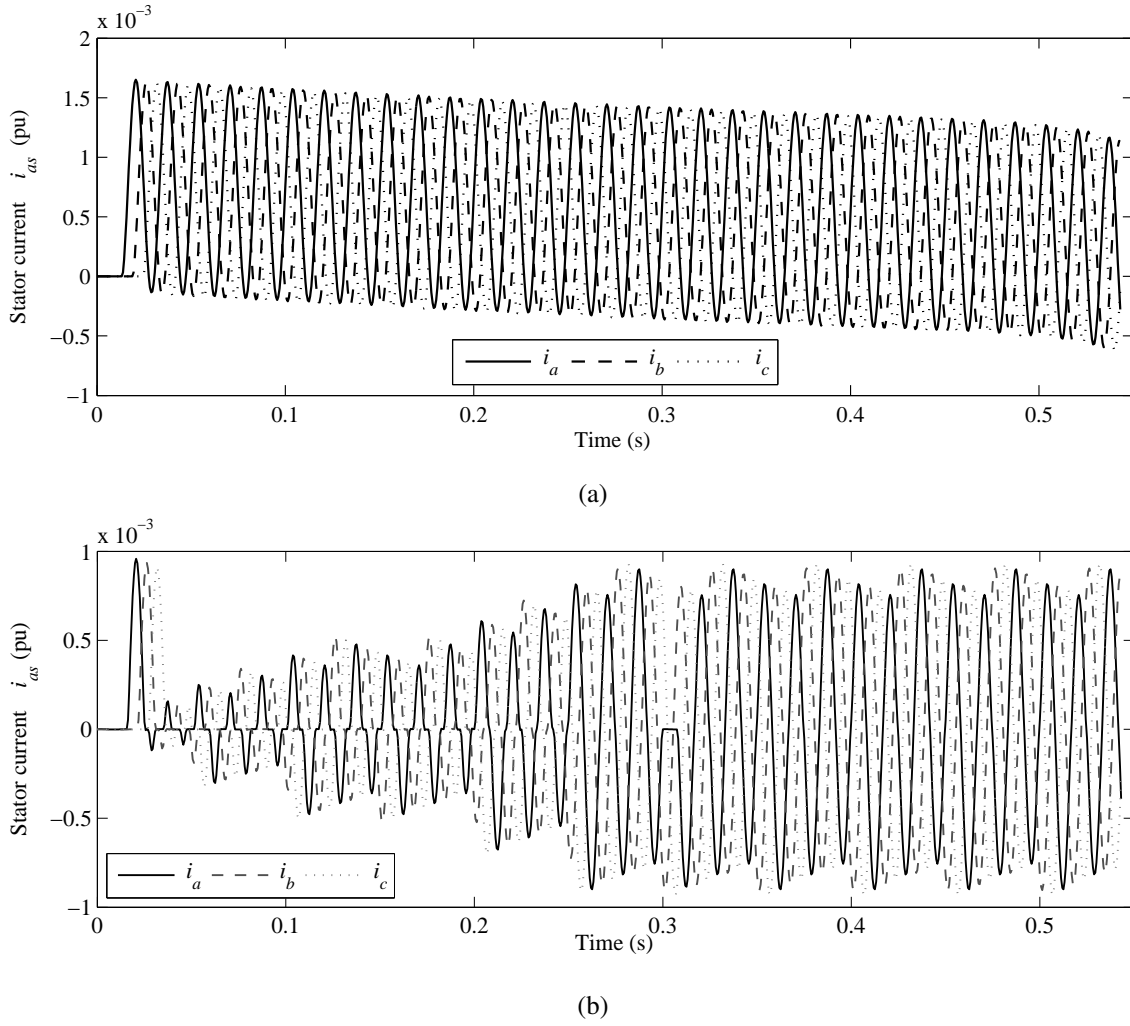


Fig. 8. Current at the stator of the IM  $I_{53}$  (pu): (a)stand alone and (b)AC voltage control.

decremented until the motor accelerates or the current limit is not seen. The end of the optimal soft start is identified with the fall of voltage across the nonconducting thyristor to a value below 80% of the value when the motor is at standstill. It is worth to say that the decrease of the fire angle can be done smoother, but for illustration purposes a decrement by  $3^\circ/\text{cycle}$  was selected. Also, empiricism is needed in choosing the value of 80%. Fig. 7 depicts the optimal AC voltage soft-start controlled diagrammatically.

Due that the main solution is conducted in FD, harmonics/interharmonics can be directly extracted from the solution variables without the need of post-processing. Fig. 10 shown the harmonic content of the current through the stator  $I_{53}$  obtained during the dynamic-state (when the fall of the voltages across the SCR is equal or less than 20%). The harmonic content were normalized with respect to the fundamental frequency.

#### IV. CONCLUSIONS

In this paper, a hybrid frequency-time domain methodology has been used to dynamic state. The network includes an undersea power cable, an AC voltage control based SCR,

an induction machine, and linear loads. The methodology is based on numerical Laplace transform and Norton (Thevenin) equivalents. Although nonlinear elements are solved in local TD procedure. The main characteristics of the methodology used in this this network are:

- FDE leads to partition the network in N subnetworks.
- Nonlinear elements are taken in the main program obtained the Jacobians by a time domain local procedure.
- Controls and nonlinearities have been implemented without further details than the elements themselves.
- One can move deeper into each subnetwork for calculating any internal variable under interest.
- The fact that the numerical Laplace transform and the DFT are related, allows obtaining either steady or transient states with a minor modification to the solution algorithm.
- Harmonics and interharmonics can be directly extracted from the solution variables without post-processing.
- The methodology can be potentially used in large networks, where the dynamics of specifics machines are under study. Particularly at the start of the machines.

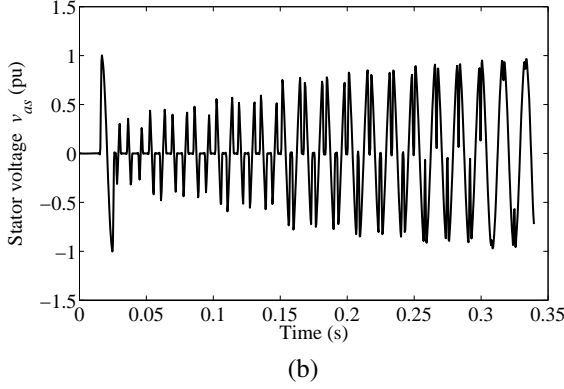
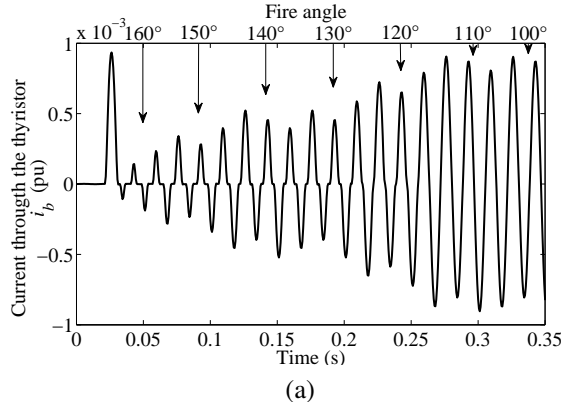


Fig. 9. AC voltage control parameters phase  $b$  : (a) Current through the SCR  $i_{SCR2}$  and (b) stator voltage  $v_{as}$ .

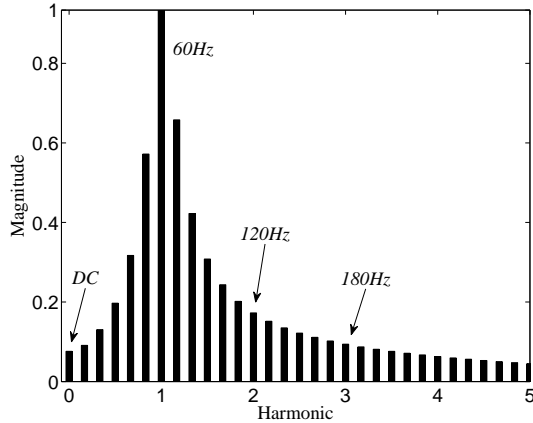


Fig. 10. Harmonic content of the current  $I_{33}$  during steady state.

- Although in this work is presented a very basic control, the methodology can allow more sophisticated control with a minor changes.

#### APPENDIX A NUMERICAL LAPLACE TRANSFORM

Linear and frequency dependent elements are represented as a frequency domain equivalent to obtain the solution of the entire network. The direct and inverse numerical Laplace transforms are given by:

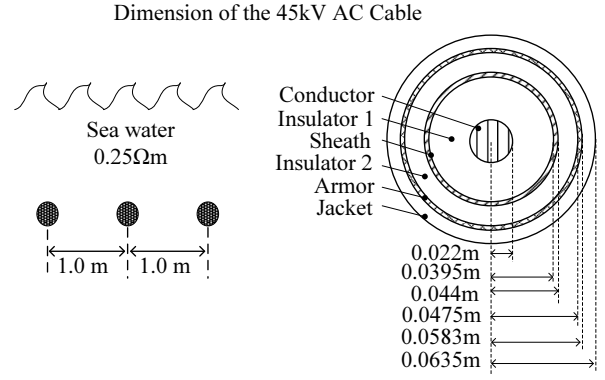


Fig. 11. Undersea Power cable cross section and its geometrical arrangement.

$$F_k = \Delta t \sum_{n=0}^{N-1} f_n \exp^{-cn\Delta t} \exp^{-j2\pi kn/N}, k = 0, 1, \dots, N-1, \quad (9)$$

and

$$f_n = \frac{\exp^{cn\Delta t}}{\Delta t} \text{Re} \left\{ F_k \sigma_k \exp^{j2\pi kn/N} \right\}, n = 0, 1, \dots, N-1, \quad (10)$$

where:

$$f_n \equiv f(n\Delta t), \quad \text{for } n = 0, 1, \dots, N-1, \quad (11a)$$

$$f_k \equiv \begin{cases} F(c + jk\Delta\omega), & k = 0, 1, \dots, N/2 \\ F[c + j(k-N)\Delta\omega], & k = N/2 + 1, \dots, N-1 \end{cases} \quad (11b)$$

$$\Delta t = T/N, \quad (11c)$$

$$\Delta\omega = 2\Omega/N = 2\pi/T. \quad (11d)$$

where  $\sigma$  is a data window. It is worth mention that Eq. 9 and Eq. 10 are the NLT using regular sampling. For this work, the Hannin data window was chosen. Also  $c$  represents the damping factor taken by using Wedepohl's criterion  $c = \ln(N^2)/T$ . By using a Matlab program one can implement the *ifft/fft* routines for Eq. 9 and Eq. 10. For further details about the numerical Laplace transform please refer to [8].

#### APPENDIX B POWER CABLE GEOMETRICAL CONFIGURATION

Undersea power cable geometrical configuration used in the case of study is presented in Fig. 11 where it is shown the cross section and the distance between phases.

#### APPENDIX C LINEAR ELEMENTS DATA

- Transformers:  $R = 1\Omega$  and  $L = 1H$ .
- linear load:  $R = 100\Omega$  and  $L = 1H$ .
- Induction machine:  $R_s = 0.3\Omega$ ,  $L_s = 1.5H$ ,  $R_r = 0.6\Omega$ ,  $L_r = 1.5H$ , and  $L_m = 26H$ .

#### REFERENCES

- [1] H. W. Dommel, *Electromagnetic Transients Program Reference Manual (EMTP theoretic book)*, Portland, OR: Bonneville Power Administration, 1986.

- [2] A. Ramirez, "Frequency-domain computation of the steady and dynamic states including nonlinear elements", *IEEE Trans. on Power Delivery*, vol. 24, no. 3, July 2009, pp. 1609-1615.
- [3] J. J. Chavez, A. Ramirez, V. Dinavahi, R. Iravani, J. Martinez, J. Jatskevich, and G. Chang. "Interfacing techniques for time-domain and frequency-domain simulations methods", *IEEE Trans. on Power Delivery*, vol. 25, no. 3, July 2010, pp. 1796-1807.
- [4] T. M. Rowan and T. A. Lipo, "A qualitative analysis of induction motor performance improvement by SCR voltage control", *IEEE Trans. on Industry Applications*, vol. IA-19, no. 4, July/August 1983, pp. 545-553.
- [5] L. M. Wedepohl and D. J. Wilcox "Transient analysis of underground power- transmission system", *Proceedings on IEE*, vol. 120, no. 2, February 1973, pp. 253-260.
- [6] L. Marti, "Simulation of transients in underground cables with frequency-dependent modal transformation matrices", *IEEE Trans. on Power Delivery*, vol. 3, no. 3, July 1988, pp. 1099-1110.
- [7] V. V. Sastry, M. Prasad, and T. V. Sivakumar, "Optimal soft starting of voltage-controller-fed IM drive based on voltage across thyristor", *IEEE Trans. on Power Electronics*, vol. 12, no. 6, November 1997, pp. 1041-1051.
- [8] P. Moreno and A. Ramirez, "Implementation of the numerical Laplace transform: a review", *IEEE Trans. on Power Delivery*, vol. 23, no. 4, October 2008, pp. 2599 - 2609 .